



Published in final edited form as:

Am J Physiol Regul Integr Comp Physiol. 2005 September ; 289(3): R851–R861.

THE RESPONSE OF MEMBRANE POTENTIAL (V_m) AND INTRACELLULAR pH (pH_i) TO HYPERCAPNIA IN NEURONS AND ASTROCYTES FROM RAT RETROTRAPEZOID NUCLEUS (RTN)

Nick A. Ritucci¹, Joseph S. Erlichman², J.C. Leiter³, and Robert W. Putnam¹

¹Department of Neuroscience, Cell Biology and Physiology, Wright State University School of Medicine, 3640 Colonel Glenn Highway, Dayton, OH 45435; ²Department of Biology, St. Lawrence University, 10 Ramoda Drive, Canton, N.Y. 13627; and ³Department of Physiology, Dartmouth Medical School, One Medical Center Drive, Lebanon, N.H. 03756

Abstract

We compared the response to hypercapnia (10%) in both neurons and astrocytes between a distinct area of the retrotrapezoid nucleus (RTN), the medio-caudal RTN (mcRTN) and more intermediate and rostral RTN areas (irRTN) in medullary brain slices from neonatal rats. Exposure to hypercapnic acidosis (HA) caused pH_o to decline from 7.45 to 7.15 and caused a maintained, intracellular acidification of 0.15 ± 0.02 pH unit in 90% of neurons from both areas of the RTN ($n=16$). HA excited 44% of mcRTN (7 of 16) and 38% of irRTN neurons (6 of 16), increasing firing rate by $167 \pm 75\%$ (chemosensitivity index, CI, of $256 \pm 72\%$) and $310 \pm 93\%$ (CI of $292 \pm 50\%$) respectively. These responses did not vary throughout neonatal development. We investigated the role of pH_o by comparing the responses between HA (decreased pH_i and pH_o) and isohydric hypercapnia (IH; decreased pH_i with constant pH_o) in mcRTN neurons. Neurons excited by HA (firing rate increased by $156 \pm 46\%$; $n=5$) were excited to the same extent by IH (firing rate increased by $167 \pm 38\%$; $n=5$). Neurons insensitive to HA were also insensitive to IH. In astrocytes from both areas of the RTN, exposure to HA caused a maintained, intracellular acidification of 0.17 ± 0.02 pH unit ($n=6$) and a depolarization of 5 ± 1 mV ($n=12$). In summary, a high percentage of neurons (42%) from the entire RTN are highly responsive (CI 248%) to HA; this may reflect both synaptically driven and intrinsic mechanisms of CO_2 sensitivity. Changes of pH_i appear to be a more significant stimulus than changes of pH_o in chemosensory RTN neurons. Finally, the lack of astrocytic pH_i regulation in response to HA suggests that astrocytes do not enhance extracellular acidification during hypercapnia in the RTN in the neonatal period.

Keywords

brainstem; chemosensitivity; extracellular pH; glia; ventilatory control

INTRODUCTION

Central CO_2 chemosensitivity resides in multiple regions of the brainstem (for reviews see 30,46). One of these regions, the retrotrapezoid nucleus (RTN), is located within Mitchell's chemosensitive area of the rostral ventrolateral medulla. The RTN was identified as a nucleus a little over a decade ago (42,57). The involvement of this region in the control of breathing

was shown by lesioning the RTN, which decreased the ventilatory response to CO₂ (1,32,33, 34). Ventilation also increased when the RTN was exposed to hypercapnic solutions (21,25, 26).

The mechanism of CO₂ chemosensitivity in RTN neurons (and other neurons from chemosensitive regions for that matter) is still unknown. There are very few studies of intracellular activity from cells in the RTN. In the first intracellular recordings within the region now known as the RTN, it was found that lowering the HCO₃⁻ concentration in a CO₂/HCO₃⁻ buffered medium increased the firing rate of neurons (37). Only two previous studies (excluding this one) have investigated the mechanism of CO₂-chemosensitivity in individual RTN neurons (29,36).

Carbon dioxide is a major stimulus to breathing. When the CO₂ level rises, the concentrations of both dissolved CO₂ and HCO₃⁻ increase (both intra- and extracellularly) and intracellular pH (pH_i) and extracellular pH (pH_o) decrease. Any one of these changes might alter neuronal activity, but the change in pH_i seems most important (16,63). However, the exact stimulus for central CO₂ chemosensitivity has remained elusive (39). A number of findings have suggested that inhibition of K⁺ channels by decreases in pH_i and/or pH_o is the most likely mechanism of neuronal activation by CO₂ (9,16,47,65,67,68). The activation of Ca²⁺ channels may also be involved in chemosensitive signaling (17). The actual mechanism of CO₂ chemosensitivity most likely involves multiple signaling and ionic processes (15,46,50).

Since changes in pH are thought to play such a critical role in CO₂ chemosensitivity, simultaneous measurement of V_m and pH_i of cells in chemosensitive regions provide a powerful technique to determine the mechanism(s) of chemosensitivity. Such studies have recently been done in another chemosensitive area, the locus coeruleus (16) and the neural activity of cells within the locus coeruleus was best correlated with changes in pH_i. In the current study, we simultaneously measured V_m and pH_i in individual neurons of the RTN to characterize their CO₂ chemosensitivity. Recently, the medio-caudal area of the RTN (comprised of approximately 300 neurons) was tentatively identified as the site of the ventral medullary chemoreceptors first identified in the early 1960's (26,29). This suggestion is at odds with evidence that indicates the entire RTN is involved in the control of breathing (6, 21,23,24,25,31,33,36,37,55,60). Therefore, we chose to divide the RTN into two areas to determine if there were differences in the response to hypercapnia of neurons within each area: the medio-caudal area discussed above, and more intermediate and rostral areas of the RTN. The mechanism of CO₂ chemosensitivity in medio-caudal RTN neurons has recently been suggested to involve inhibition of a TASK channel (29). TASK channels are inhibited by decreased pH_o, and we exposed medio-caudal RTN neurons to both hypercapnic acidosis (decreased pH_i and pH_o) and isohydric hypercapnia (decreased pH_i and constant pH_o) to assess the possible role of TASK channels in chemosensory neurons from the RTN.

There is evidence that suggests that astrocytes may be involved in CO₂ chemosensitivity (14, 18,20). The role that astrocytes play in the central nervous system is much more extensive than once thought, and includes the control and regulation of many substances in the extracellular space, such as glutamate, K⁺ and H⁺ (11,22,48). It has been proposed that astrocytes contribute to the mechanism of CO₂ chemosensitivity by acidifying the extracellular environment during hypercapnia, and thereby, magnifying the signal to the central chemoreceptors (14,20). We studied this possibility by simultaneously measuring the responses of V_m and pH_i to hypercapnic acidosis in RTN astrocytes.

Preliminary reports of these findings have been published previously (47,52).

MATERIALS AND METHODS

Solutions and materials.

Control solution contained (in mM): 124 NaCl, 3 KCl, 1.2 NaH₂PO₄, 1.3 MgSO₄, 2.4 CaCl₂, 26 NaHCO₃, and 10 glucose and was equilibrated with either 5% CO₂/95% O₂ (pH ~ 7.45 at 37° C) or 10% CO₂/90% O₂ (hypercapnic solution; pH ~ 7.15 at 37° C). For the isohydric hypercapnic solution, NaHCO₃ was increased to 52mM (isosmotically replacing NaCl) and equilibrated with 10% CO₂/90% O₂ (pH ~ 7.45 at 37° C). The pH_i calibration solution contained (in mM): 127 KCl, 1.2 KH₂PO₄, 1.3 MgSO₄, 2.4 CaCl₂, 26 K-HEPES (N-2-hydroxyethylpiperazine-N'-2-ethanesulfonic acid), 10 glucose, and 0.004 nigericin (pH 7.4 at 37° C). Nigericin was purchased from Sigma and was added from a 16.7 mM stock solution (in DMSO). Pyranine (8-hydroxypyrene-1,3,6-trisulfonic acid) was purchased from Molecular Probes and was added from a 4 mM stock solution (in water). Fluo-4 was also purchased from Molecular Probes and prepared as a 5 mM stock solution (in DMSO), which was then added to control solution at a final concentration of 5 μM.

Preparation of medullary brain slices.

Transverse brain slices (200–300μm) were prepared from preweanling Sprague-Dawley rats (postnatal day, P0–P17) beginning at the most caudal level of the facial nucleus and extending rostrally for ~ 600 to 900 μm (Fig. 1). Slices were cut into ice-cold control solution using a vibratome (Pelco 101, series 1000) and subsequently stored at room temperature. Experiments began at least one hour after slicing. Individual slices were placed in a superfusion chamber (~ 1.0 ml volume), which was on the stage of an upright Nikon Eclipse E600 microscope, immobilized with a grid of nylon fibers, and superfused at ~ 4 ml/min with control solution (37° C).

Visualization of brain slices.

Individual RTN neurons and astrocytes were visualized using infrared video microscopy. A 60X water immersion objective (W.D. 3 mm; N.A. 0.8) was used during these experiments and equipped with Hoffman Modulated Contrast optics. Light was directed to a Nikon multi-image port module equipped with a 505 nm dichroic mirror, which allowed 100% of the infrared image and 100% of the fluorescence image (see below) to each port simultaneously. The infrared image was then directed to a Sony CCD-IRIS video camera and displayed on a Sony video monitor.

Imaging of pyranine-loaded slices.

The pH-sensitive dye, pyranine, was loaded into individual RTN neurons and astrocytes with whole-cell pipettes (see below). Pyranine-loaded cells were excited (with light from a xenon arc lamp) alternately at 450 ± 10 nm (pH-sensitive) and 415 ± 10 nm (pH-insensitive) wavelengths using a Sutter Lambda 10–2 filter wheel. An acquisition took about 2 seconds and was repeated at 20 to 60 second intervals. There was no excitation light between acquisitions. Emitted fluorescence at 515 ± 10 nm (all filters from Omega Optical) was directed to the Nikon multi-image port module and then directed to a GenIIsys image intensifier and a CCD100 camera (both from Dage-MTI). The subsequent fluorescence images were collected and processed using Metafluor 4.6r5 software (Universal Imaging), and the 450/415 fluorescence ratios (R_{fl}) determined. At the end of each experiment, we performed a one point calibration at pH 7.4 using a high K⁺/nigericin calibration solution. This allowed us to normalize the R_{fl} values (N_{fl}) and convert N_{fl} into pH_i using the following calibration equation from previous studies (28,53):

$$\text{pH}_i = 7.5561 + \log(N_{fl} - 0.1459) / (2.0798 - N_{fl}).$$

Fluo-4 loading of slices.

The fluorescent dye, fluo-4, is preferentially loaded by glia (43). Therefore, slices were loaded with fluo-4 to aid identification of astrocytes. Slices were incubated in control solution containing 5 μ M of the membrane permeant form of fluo-4, fluo-4 AM, for one hour in the dark at 37 $^{\circ}$ C. Slices were subsequently washed and stored in fresh, control solution at room temperature until experiments began (i.e. at least a 30 minute wash time). Fluo-4 fluorescence was imaged by exciting the dye at 490nm and collecting the emitted fluorescence at 520nm. Fluo-4 fluorescence did not interfere with pyranine fluorescence: fluo-4 fluorescence was absent when imaging with our pyranine emission cube (data not shown). In later experiments, astrocytes were visually identified without fluo-4 loading.

Whole-cell recordings.

Whole-cell pipettes (5 M Ω) were fabricated from borosilicate glass (TW150-3, World Precision Instruments) using a Narishige PP-830 dual stage pipette puller and were filled with a solution containing (in mM): 130 K-gluconate, 1 MgCl₂, 10 HEPES, 0.4 EGTA (ethylene glycol-bis(β -aminoethyl ether)-N, N, N', N'-tetraacetic acid), 2 Na₂ATP, 0.3 Na₂GTP and 0.2 pyranine (pH \sim 7.35 at 37 $^{\circ}$ C). This filling solution, which has no added Ca²⁺ and low levels of EGTA reduces washout in chemosensitive neurons (7,17). The pipette holder contained a Ag-AgCl wire and the circuit was completed with a Ag-AgCl wire placed (downstream to the brain slice) in the superfusion bath. Slight positive pressure was applied to the whole-cell recording pipette. To achieve a tight seal, the pipette was initially manipulated to touch the membrane of the soma. Tight seals were attempted solely on the outer edge of the soma, so that the fluorescence from pyranine in the pipette would not interfere with the fluorescence of pyranine in the soma. Once the pipette touched the outer edge of the soma, negative pressure was applied to the pipette to form a tight (GigaOhm) seal with the cell membrane. The tight seal was then ruptured to achieve the whole-cell configuration. Pyranine diffused from the whole-cell pipette into the cell and stable R_{fl} values were achieved within about 15 minutes (28).

Perforated-patched recordings.

Pipettes (5 M Ω) were fabricated from borosilicate glass (TW150-3, World Precision Instruments) using a Narishige PP-830 dual stage pipette puller and contained (in mM): 130 K-methanesulfonate, 20 KCl, 5 HEPES, 1 EGTA, 240 μ g/ml amphotericin B (pH \sim 7.35 at 37 $^{\circ}$ C). The pipette was backfilled with this solution, while the tip of the pipette was filled with an amphotericin B free solution. Amphotericin B was purchased from Sigma and was added from a 60mg/ml stock solution (in DMSO).

Electrophysiological recordings were conducted in current clamp mode, and V_m was measured with a Dagan BVC-700 amplifier. As such, V_m represents a time-averaged value of all potentials and was averaged over at least a 1 minute period using pClamp software. A healthy neuron had a resting V_m of between -30mV and -60mV. All neurons were spontaneously active. A healthy astrocyte had a resting V_m of between -70mV and -80mV, and action potentials could not be evoked upon injection of depolarizing currents.

Data analysis

V_m was saved to both a digital VCR (Vetter, model 400) and to Axoscope software (version 8.0) for later analysis. Firing rates were determined (10 sec bins) using a window discriminator/integrator (Winston Electronics) and were determined by averaging firing rate values over at least a 1 minute period just before switching to a new solution. We expressed the magnitude of chemosensitivity by calculating the chemosensitivity index (CI), as described by Wang et al. (64). CI was calculated for the response of each neuron and then averaged across all neurons.

The original calculation of CI is based on a change of pH_o of 0.2 pH unit (64). Since we use HA conditions that result in a change of pH_o of 0.3 pH unit, we adjusted our calculated CI based on a change of 0.2 pH unit so that it would be directly comparable to CI values calculated for chemosensitive neurons from other brainstem regions (46,64). A value for CI cannot be calculated when using isohydric hypercapnia (since there is no change in pH_o). Therefore, we also expressed the % by which firing rate (FR) increased in each condition according to the equation: % FRincrease = $[(FR_{hypercapnia} - FR_{control})/FR_{control}] \cdot 100$. All values are given as the mean \pm 1 standard error of the mean (SEM). Significant differences between 2 means were determined by Student's paired *t* tests (significance at $P < 0.05$) and the distribution of % chemosensitive neurons was compared with a χ^2 test.

RESULTS

Whole-cell recordings of RTN neurons during hypercapnic acidosis.

All recordings of RTN neurons and astrocytes were performed on cells that were no deeper than 200 μ m from the ventral surface and were typically one focal plane below the slice surface. We studied two populations of RTN neurons (Fig. 1, modified from 41). One small population (~ 300 cells) lies in the most caudal slice through the RTN (i.e. bregma 11.7 – 11.4) and is directly ventral and at the medial aspect of the facial nucleus (29). This area is well vascularized and the presence of vessels aided in its identification. We refer to this area as the medio-caudal RTN (mcRTN). The other population of neurons lies in more intermediate and rostral slices (i.e. bregma 11.4 – 10.5), and therefore will be referred to as the irRTN.

Firing rate, V_m and pH_i were measured in neurons from the mcRTN in the whole-cell configuration (Fig. 2). Slices were initially superfused with control solution until stable values of firing rate, V_m and pH_i were achieved. Upon superfusion with hypercapnic acidosis solution, 3 of 8 neurons (38%) increased their firing rate from an initial value of 0.90 ± 0.38 Hz (range 0.2 to 1.5 Hz) to 2.8 ± 0.44 Hz, which corresponds to a CI of $314 \pm 147\%$. These three neurons also depolarized ~ 6 mV, from an initial value of -45.0 ± 1.7 mV (range -42 to -48 mV) to -38.8 ± 0.9 mV. In addition, there was a maintained intracellular acidification of 0.12 pH unit, from an initial value of 7.31 ± 0.01 to 7.19 ± 0.02 . Upon return to control solution, firing rate (0.73 ± 0.27 Hz), V_m (-46 ± 2.1 mV) and pH_i (7.30 ± 0.02) returned towards their initial values. In the other 5 neurons tested (Fig. 3), there was once again a maintained intracellular acidification during hypercapnic acidosis, from an initial value of 7.32 ± 0.01 to 7.20 ± 0.01 . However, these neurons did not exhibit a change in firing rate (from 1.54 ± 0.41 Hz (range 0.2 to 3.0 Hz) to 1.54 ± 0.41 Hz) or V_m (from -43.6 ± 2.0 mV (range -38 to -50 mV) to -42.4 ± 2.2 mV). Upon return to control solution, pH_i returned to its initial value (7.31 ± 0.02). Firing rate (1.54 ± 0.41 Hz) and V_m (-43.4 ± 1.4 mV) remained unchanged.

Firing rate, V_m and pH_i were also measured in neurons from the irRTN, using whole-cell pipettes. In 2 of 8 neurons (25%), there was an increase in firing rate upon exposure to hypercapnic acidosis from an average initial value of 0.65Hz (range 0.3 to 1.0 Hz) to 4.0Hz, which corresponds to a CI of $413 \pm 149\%$. In addition, these neurons depolarized ~ 3mV, from an average initial value of -46.6 mV (range -37 to -52 mV) to -43.5 mV. There was also a maintained, intracellular acidification of 0.17 pH unit, from an average initial value of 7.29 to 7.12. Upon return to control solution, average firing rate (1.0Hz), V_m (-42.0 mV) and pH_i (7.26) returned back towards their initial values. In the other 6 neurons tested, firing rate (from 1.45 ± 0.731 Hz (range 0.2 to 5.0 Hz) to 1.45 ± 0.73 Hz) and V_m (from -44.8 ± 1.8 mV (-41 to -52 mV) to -45.7 ± 3.2 mV) remained unchanged. However, there was once again a maintained, intracellular acidification during hypercapnic acidosis from an initial value of 7.34 ± 0.03 to 7.20 ± 0.09 . Upon return to control solution, pH_i returned back to its initial value (7.29 ± 0.07) and firing rate (1.37 ± 0.65 Hz) and V_m (-42.5 ± 4.3 mV) again remained unchanged.

Perforated-patch recordings of RTN neurons during hypercapnic acidosis.

Since whole-cell pipettes can cause washout of soluble intracellular components, which could be important in the signaling mechanism of CO₂ chemosensitivity (10,17,49), we repeated the experiments using perforated-patch recordings, which avoided issues of washout of the V_m response to hypercapnia. Firing rate and V_m were measured in neurons from the mcRTN, using perforated-patch pipettes. Slices were initially superfused with control solution until stable values of firing rate and V_m were achieved. Upon superfusion with hypercapnic acidosis solution, 4 of 8 neurons (50%) increased their firing rate from an initial value of 2.0 ± 0.87 Hz (range 0.3 to 4.0 Hz) to 4.7 ± 1.5 Hz, which corresponds to a CI of $210 \pm 36\%$. These neurons also depolarized ~ 5 mV, from an initial value of -42.7 ± 6.3 mV (range -34 to -55 mV) to -37.3 ± 5.8 mV. Upon return to control solution, firing rate (2.3 ± 0.73 Hz) and V_m (-39.3 ± 6.0 mV) returned towards their initial values. In the other 4 neurons tested, there was no change in firing rate (from 2.40 ± 0.47 Hz (range 1.0 to 3.0 Hz) to 2.38 ± 0.47 Hz) or V_m (from -34.5 ± 5.4 mV (range -33 to -46 mV) to -38.5 ± 4.3 mV) during exposure to hypercapnic acidosis. Upon return to control solution, firing rate (2.0 ± 0.41 Hz) and V_m (-36.8 ± 5.7 mV) remained unchanged.

Firing rate and V_m were also measured in neurons from the irRTN, using perforated-patch pipettes. In 4 of 8 neurons (50%), there was an increase in firing rate upon exposure to hypercapnic acidosis, from an initial value of 1.2 ± 0.91 Hz (range 0.2 to 4.0 Hz) to 3.7 ± 2.7 Hz, which corresponds to a CI of $241 \pm 26\%$. These neurons depolarized ~ 4 mV, from an initial value of -39.7 ± 4.5 mV (range -38 to -46 mV) to -36.0 ± 5.5 mV. Firing rate (0.9 ± 0.6 Hz) and V_m (-38.0 ± 7.4 mV) returned towards their initial values under control conditions. In the other 4 neurons tested, firing rate (from 1.5 ± 0.35 Hz (range 0.5 to 3.0 Hz) to 1.3 ± 0.35 Hz) and V_m (from -42.3 ± 4.8 mV (range -32 to -55 mV) to -44.3 ± 4.0 mV) remained unchanged during hypercapnic acidosis exposure and upon return to control solution (firing rate of 1.3 ± 0.35 Hz and V_m of -40.0 ± 5.0 mV).

Age effects on chemosensitivity of RTN neurons.

There could be concerns that our findings are confounded by developmental changes in RTN neuronal chemosensitivity in the neonatal rats used in this study. Thus, we examined the CO₂ sensitivity of all excited neurons (regardless of method of study and location within the RTN) from our neonatal rats (P0–P17). All neurons studied were divided into being from rats either younger than P10 or older than P10. The percentage of neurons activated by hypercapnia from rats younger than P10 was 40% (10 activated out of 25 studied), and it was 42% (8 activated out of 19 studied) in neurons from rats older than P10. These values are not significantly different ($P > 0.12$). The remainder of the neurons did not respond to hypercapnia with a change in firing rate. We did not observe any RTN neurons whose firing rate was inhibitable by hypercapnia. We also calculated the CI of the neurons from the different age groups to determine their relative chemosensitivity. The CI of neurons activated by CO₂ was $209 \pm 13\%$ in animals less than P10 and $296 \pm 65\%$ in animals older than P10. These values are also not significantly different ($P > 0.1$). Thus, chemosensitive neurons in the RTN do not appear to show developmental changes in their chemosensitivity during postnatal development.

Whole-cell recordings of RTN neurons during isohydric hypercapnia.

Since pH_o has been suggested to play a role in the response of RTN neurons to hypercapnia (29), we exposed the slices to both hypercapnic acidosis (which results in a decrease in both pH_i and pH_o) and isohydric hypercapnia (which results in a decrease in pH_i with a constant pH_o), while measuring V_m and pH_i using whole-cell pipettes (Fig. 4). These experiments were performed solely in the mcRTN. Slices were initially superfused with control solution until stable values of firing rate, V_m and pH_i were achieved. Upon superfusion with hypercapnic acidosis solution, 5 of 11 neurons (45%) increased their firing rate by $156 \pm 46\%$ from an initial

value of 1.5 ± 0.35 Hz (range 0.5 to 2.5 Hz) to 3.4 ± 0.68 Hz (Fig. 4). These neurons also depolarized ~ 3 mV, from an initial value of -43.5 ± 5.2 mV (range -39 to -48 mV) to -40.4 ± 4.5 mV. In addition, there was a maintained intracellular acidification of 0.15 pH unit, from 7.31 ± 0.01 to 7.16 ± 0.02 (Fig. 4). Upon return to control solution, firing rate (1.9 ± 0.43 Hz), V_m (-44.0 ± 3.0 mV) and pH_i (7.30 ± 0.02) returned to their initial values. Slices were then superfused with isohydric hypercapnic solution. The 5 neurons that were excited by hypercapnic acidosis, were also excited by isohydric hypercapnia (Fig. 4). Firing rate increased by $167 \pm 38\%$ from 1.9 ± 0.43 Hz to 4.8 ± 1.09 Hz (Fig. 4). These neurons also depolarized ~ 3 mV, from -44.0 ± 3.0 mV to -41.2 ± 3.5 mV. The pH_i response consisted of an initial decrease of 0.10 ± 0.02 pH unit, from an original value of 7.30 ± 0.01 to 7.20 ± 0.03 , that was followed by pH_i recovery (Fig. 4). Upon return to control solution, firing rate (1.9 ± 0.57 Hz) and V_m (-44.5 ± 3.5 mV) returned to their initial values, while pH_i overshot its initial value to a value of 7.35 ± 0.02 , which is consistent with pH_i recovery. A comparison of these 5 neurons showed that their firing rate response to hypercapnic acidosis ($156 \pm 46\%$) did not differ significantly ($P > 0.85$) from their firing rate response to isohydric hypercapnia ($167 \pm 38\%$).

In the remaining 6 neurons tested (Fig. 5), there was once again a maintained intracellular acidification of 0.15 pH unit during hypercapnic acidosis, from an initial value of 7.29 ± 0.01 to 7.14 ± 0.02 . However, these neurons did not exhibit a change in firing rate (from 1.3 ± 0.55 Hz (range 0.2 to 3.5 Hz) to 1.3 ± 0.85 Hz) or V_m (from -42.3 ± 4.8 mV (range -36 to -48 mV) to -42.0 ± 5.1 mV) during hypercapnic acidosis exposure. Upon return to control solution, pH_i returned towards its initial value (7.28 ± 0.02). Firing rate (1.5 ± 0.62 Hz) and V_m (-41.8 ± 4.9 mV) remained unchanged. During exposure to isohydric hypercapnia, the pH_i response consisted of a decrease of 0.10 ± 0.03 pH unit, from an initial value of 7.28 ± 0.01 to 7.18 ± 0.03 , that was followed by pH_i recovery (Fig. 5). These neurons, again, did not exhibit a change in firing rate (from 1.5 ± 0.62 Hz to 1.6 ± 0.55 Hz) or V_m (from -41.8 ± 4.9 mV to -42.0 ± 5.1 mV) during exposure to isohydric hypercapnia. Upon return to control solution, firing rate (1.4 ± 0.72 Hz) and V_m (-42.1 ± 4.9 mV) remained unchanged, while pH_i overshot its initial value to a value of 7.36 ± 0.02 (Fig. 5), which is consistent with pH_i recovery.

Chemosensitivity in RTN neurons.

To characterize the chemosensitivity of RTN neurons we pooled our data from various regions, techniques and ages, and determined the % of neurons that responded to hypercapnia with an increased firing rate (no neuron was found to be inhibited by hypercapnia) and the magnitude of their response (as determined by the CI). In all cases, the % of neurons that responded to hypercapnic acidosis did not differ significantly with region, measuring technique or age. Thus, pooling all data, we found that 18 of a total 43 RTN neurons, or 42%, responded to hypercapnic acidosis with an increased firing rate ($>20\%$). Further, the magnitude of the response (i.e. the CI) of the 18 chemosensitive RTN neurons was $248 \pm 30\%$. These values are then the best estimates for the % of RTN neurons that are chemosensitive and the magnitude of their response to hypercapnia.

Fluo-4 loading.

To aid in the identification of astrocytes, we loaded slices with the fluorescent dye, fluo-4 (Fig. 6). Loaded cells were either spherical or irregularly shaped and were approximately $10\mu\text{m}$ in size. The loaded-cells of interest were visualized no deeper than $200\mu\text{m}$ from the ventral surface (Fig. 6) and were typically one focal plane below the slice surface. Once a fluo-4 loaded cell was identified and so assumed to be an astrocyte, electrophysiological recordings were performed (see below). Every fluo-4 loaded cell met our electrophysiological criteria for astrocyte (see *Whole-cell recordings of RTN astrocytes during hypercapnic acidosis*). Once we became proficient at identifying astrocytes, fluo-4 loading was no longer necessary.

Whole-cell recordings of RTN astrocytes during hypercapnic acidosis.

We also wanted to see what the effect of hypercapnic acidosis was on the V_m and pH_i of astrocytes from both the mcRTN and irRTN. Our criteria for confirming that we were patched on an astrocyte were: silent cells with a highly negative V_m , the inability to evoke an action potential with depolarizing current injection, and the appearance of depolarization-induced alkalization (Fig. 7). All cells that we patched that lacked the ability to generate action potentials also had a highly negative V_m and exhibited depolarization-induced alkalization. Because the changes seen in V_m and pH_i during exposure to hypercapnic acidosis were the same in both areas while using whole-cell pipettes, the data ($n = 6$) from both areas were pooled. Astrocytes, like neurons, acidified by 0.15 pH unit (from 7.32 ± 0.02 to 7.17 ± 0.02) and maintained that acidification the entire duration of the exposure to hypercapnic acidosis (Fig. 7). The membrane potential of astrocytes, which was far more hyperpolarized than the resting V_m of neurons, also depolarized in response to hypercapnic acidosis by ~ 4 mV from an initial value of -75.0 ± 1.4 mV to -70.6 ± 1.8 mV. Upon return to control solution, pH_i returned towards its initial value (7.31 ± 0.06), as did V_m (-72.2 ± 3.1 mV) (Fig. 7). At the end of each of these experiments, we wanted to further confirm these recordings were from astrocytes, so we depolarized the membrane with approximately +40 mV DC current and observed the change in pH_i . It has been shown in a previous study, that depolarizing astrocytes will cause the inwardly-driven electrogenic $Na^+-HCO_3^-$ cotransporter to be activated, and thus, produce an intracellular alkalization (15), termed depolarization-induced alkalization (39). This is what was seen in RTN astrocytes (Fig. 7). If these cells were neurons, the depolarization would have produced an intracellular acidification (61).

Perforated-patch recordings of RTN astrocytes during hypercapnic acidosis.

As previously stated, since whole-cell pipettes can cause washout of the neuronal electrical response to hypercapnia, we were concerned that the use of whole-cell pipettes could also alter the response of astrocytes to hypercapnia. Therefore, we repeated the whole-cell pipette experiments using perforated-patch recordings. Once again, the results in astrocytes from both RTN areas were combined ($n = 6$), since the changes seen in V_m during hypercapnic acidosis were the same. The depolarization measured with perforated-patch pipettes was similar to that observed using whole-cell pipettes. Hypercapnic acidosis resulted in a membrane depolarization of ~ 5 mV from an initial value of -77.8 ± 1.0 mV to -72.8 ± 0.7 mV. Upon return to control conditions, V_m returned towards its initial value (-77.5 ± 1.2 mV).

DISCUSSION

There were four main findings in this study. First, a similar percentage (i.e. $\sim 42\%$) of neurons were excited by hypercapnic acidosis in the mcRTN and the irRTN. Furthermore, RTN neurons from both areas, just like in other chemosensitive regions of neonates (51) had a maintained intracellular acidification during hypercapnic acidosis. Second, pH_i appears to play a major role, and decreased pH_o a lesser role, in the response of RTN neurons to hypercapnia. Every neuron from the mcRTN that was excited by hypercapnic acidosis was also excited by isohydric hypercapnia and every neuron that was insensitive to hypercapnic acidosis was also insensitive to isohydric hypercapnia. Third, the firing rate increase was large (CI $\sim 250\%$) and was the same in response to hypercapnic acidosis and isohydric hypercapnia in both the mcRTN and irRTN. Finally, the response of astrocytes to hypercapnia was shown to be similar to that of neurons: a modest depolarization (~ 5 mV) along with a maintained intracellular acidification. These data indicate that the entire RTN is equally and highly chemosensitive and that astrocytes do not appear to be regulating pH_o under conditions of hypercapnic acidosis.

Distribution of CO₂-sensitive neurons within the RTN.

The present study investigated the V_m and pH_i responses to hypercapnia of individual neurons and astrocytes of the mcRTN and irRTN in brain slices from neonatal rats. There were no consistent or significant differences in resting V_m or initial firing rate based on the method of study or location within the RTN. We found that 38% (3 of 8) of neurons from the mcRTN were excited by hypercapnic acidosis when using whole-cell pipettes and 50% (4 of 8) were excited by hypercapnic acidosis when using perforated-patch pipettes. These values are somewhat higher than the values reported by Okada et al. (36), who found that 29% of RTN neurons in the same area were excited by hypercapnic acidosis when recorded with perforated-patch pipettes. Mulkey et al. (29) also performed recordings in the medio-caudal RTN. Using loose-patch recordings in a HEPES-buffered solution, they found that 46% of neurons tested were excited by decreasing pH_o to 6.9 (control pH 7.3). A few of these neurons were also excited by hypercapnic acidosis (in a CO₂/HCO₃⁻ buffered solution), prompting the speculation that the area from which they recorded (corresponding to the mcRTN recorded in this study) might be area M of the VLM (see 26), which was first described in the early 1960s.

We also wanted to compare the CO₂-chemosensitivity of mcRTN to irRTN neurons, to see if the mcRTN represents a specialized chemosensitive area. We found that a similar percentage of mcRTN and irRTN neurons were excited by hypercapnic acidosis (~ 44% versus ~ 38%, respectively) and to the same extent (CI of $256 \pm 72\%$ and $310 \pm 65\%$, respectively). These findings suggest that the mcRTN is not particularly distinct from the rest of the RTN. This is not entirely surprising, given the fact that Mitchell's rostral chemosensitive region of the rostral ventrolateral medulla (where the RTN is located) encompasses a fairly large area (27). The RTN in particular, has been shown to be CO₂ and acid chemosensitive starting at its most caudal end and extending to its most rostral pole (6,21,23,24,25,31,33,37). In addition, increased c-fos in response to hypercapnia has been seen in the caudal to rostral extent of the RTN without any particular concentration of CO₂ responsive cells in the mcRTN (36,55,60), suggesting that much of the RTN is involved in the control of breathing.

One possible limitation of this study is that the brain slices were taken from young animals (P0–P17). Investigators study neonatal brain slices because the astrocytic proliferation, which starts about P8–P12, interferes with the access of both patch and sharp electrodes to the neurons, and because the growth of the neuropil in older animals makes imaging individual neurons within the slice difficult. However, the ventilatory response to CO₂ in neonates changes dramatically in this age range (45,58,67), and the question arises, therefore, whether these neuronal responses from neonates are representative of those from adults. We believe that they are. Our analysis of relative CO₂ sensitivity in the RTN in the current study indicates that there are no differences in chemosensitivity between neurons from rats less than P10 and those greater than P10. Furthermore, c-Fos studies indicate that the number of CO₂-responsive neurons remains constant throughout early development in the RTN (3,67). Thus, it does not appear that there are maturational changes in the CO₂ sensitivity of RTN neurons during early neonatal development.

There is one final limitation. We did not study the effect of synaptic blockade on CO₂-induced neuronal activity. Some of the neurons we studied are likely to be intrinsically CO₂ sensitive, as seen with chemosensitive neurons from other brainstem areas (8,38,49), but some of the activity that we recorded may be synaptically driven.

Intracellular pH as a chemosensory stimulus.

A decrease of pH_i is thought to play a major signaling role in CO₂ chemosensitivity (4,15,16,63). Therefore, in this study, pH_i and V_m were measured simultaneously. We also wanted to see if there was a difference in pH_i changes during hypercapnia. We found that hypercapnic

acidosis caused a maintained intracellular acidification in about 90% of the neurons in both RTN areas, which is similar to the findings of Nottingham et al. (35), although no V_m measurements were made in that study. In our study, while nearly all RTN neurons had a maintained acidification in response to hypercapnic acidosis, only about half of the neurons were found to be excited by hypercapnic acidosis. Thus, a maintained intracellular acidification cannot be used to define a chemosensitive neuron (see also 4), although all chemosensitive neurons do exhibit a maintained acidification during hypercapnic acidosis (46).

The above findings indicate that a chemosensitive neuron needs to be defined as one in which the V_m responds (either excited or inhibited) to changes in CO_2 and/or pH. This likely occurs by a change in ion channel activity. The most widely suggested chemosensitive mechanism involves inhibition of K^+ channels by a decrease in pH_i and/or pH_o during hypercapnia (9, 17,29,44,65,66,68), which would cause an increase in excitability. The K^+ channels that appear to be most sensitive to changes in pH_o are the TASK channels, and the most likely candidate would be TASK-1 with a (physiological) pK of ~ 7.4 (12). Mulkey et al. (29) speculated that TASK channels may be involved in the chemosensitive response of medio-caudal RTN neurons. However, we found that the firing rate response of medio-caudal RTN neurons was the same upon exposure to hypercapnic acidosis (both pH_i and pH_o decreased) and isohydric hypercapnia (pH_i decreased but pH_o constant). This indicates that a decrease of pH_i is sufficient to activate chemosensitive neurons in RTN and argues against inhibition of a K^+ channel (i.e. TASK-1) by a decrease in pH_o as an essential element in the mechanism of CO_2 -chemosensitivity in these neurons. Furthermore, TASK-1 expression appears to be absent in the RTN (see Fig 2B of 2). Thus, the chemosensitive response of RTN neurons is most likely mediated by other K^+ channels, perhaps including those that are sensitive to changes of pH_i .

As noted above, the firing rate response of RTN neurons to hypercapnic acidosis and isohydric hypercapnia was the same (Fig 5). However, the decrease in pH_i during isohydric hypercapnia was less than what it was during hypercapnic acidosis and it was not maintained (Fig 5). This indicates that some signal(s) other than decreased pH_i are likely involved in the chemosensitive response of RTN neurons. One possible additional signal is increased intracellular HCO_3^- concentration. Under our isohydric hypercapnic conditions, in addition to elevated CO_2 , there is a doubling of extracellular HCO_3^- concentration compared to control, which should result in elevated intracellular HCO_3^- . In another chemosensitive cell type, the glomus cell of the carotid body, elevated intracellular HCO_3^- has been shown to be involved in hypercapnia-induced excitation (59). This issue could be addressed by studying the neuronal response to metabolic acidosis (4,16). Another possible target is the activation of L-type Ca^{2+} channels which has been suggested to contribute to CO_2 chemosensitivity in locus coeruleus neurons (16). The involvement of multiple signaling pathways and targets in chemosensitive neurons in general has recently been proposed (15,46).

The study of the mechanism of CO_2 chemosensitivity has focused mainly on neurons, while the role that astrocytes might play in CO_2 chemosensitivity has largely been ignored. There is evidence that astrocytes are involved in CO_2 chemosensitivity (14,18,20). For example, perfusion of fluorocitrate (a glial toxin) into the RTN of awake rats caused an increase in the ventilatory response to CO_2 (20). We investigated the role of astrocytes in chemosensitivity by measuring the effects of hypercapnia on V_m and pH_i in astrocytes from both the mcRTN and irRTN. During hypercapnic acidosis, astrocytes behaved in the same manner as neurons: a modest depolarization ($\sim 5mV$) with a maintained intracellular acidification. Thus, astrocytes, like neurons, also do not exhibit pH_i recovery from acidification during hypercapnic acidosis despite the presence of numerous acid extruding transporters in astrocytes (56). One proposed mechanism whereby astrocytes might modify chemosensitive responses of neurons is for pH_i recovery in astrocytes in response to hypercapnia to amplify the acidification of pH_o , increasing the firing rate of chemosensitive neurons (13). Since RTN astrocytic pH_i does not

recover from hypercapnic acidification (Fig. 7), such a mechanism does not seem to be involved in the chemosensitive response of RTN neurons in the neonatal period.

Just as the RTN shows heterogeneity in neuronal properties (e.g., some cells respond to hypercapnia while others do not), there is evidence for considerable heterogeneity in astrocytes. Distinct astrocytic populations have been identified in the hippocampus based on differences in expression of AMPA-type glutamate receptors (Glu-R) and glutamate transporters (Glu-T; 62). Three populations of astrocytes can be distinguished based on the presence of different K^+ currents in caudal medullary slices from neonatal mice (19). Fukuda et al. (18) identified three populations of astrocytes based on electrophysiological measurements in ventral medullary slices from older rats during isocapnic acidosis. In 44% of astrocytes, V_m slowly depolarized by about 20 mV. In 47% of the cells, V_m was unchanged, and in 5% of the cells, V_m slowly hyperpolarized in response to decreased pH_o . Finally, we identified two distinct populations of astrocytes in brainstem slices from neonatal mice, one that regulates pH_i in response to hypercapnic acidosis and another that does not exhibit pH_i regulation (J.S. Erlichman, unpublished observation).

In the current study, we did not see evidence for heterogeneity among astrocytes. The difference between our findings and the studies discussed above may be due to the fact that we used young rats (<P20) and, in these neonatal animals, the astrocytes may not have fully differentiated into distinct populations. The degree of depolarization-induced alkalinization that we observed (Fig. 7) is about an order of magnitude smaller than values previously observed in astrocytes (39). Depolarization-induced alkalinization is largely due to activation of electrogenic Na^+ - HCO_3^- co-transport (NBC; 54). Therefore, the RTN astrocytes that we studied seem to have low NBC activity, which is consistent with the lack of pH_i recovery in response to hypercapnic acidosis (Fig. 7). It may be that the expression of NBC increases during development, and pH_i recovery might occur in older astrocytes during hypercapnic acidosis, or it may be that even in younger animals there is considerable heterogeneity among astrocytes but for whatever reason, only one type of astrocytes is readily patched.

Perspective.—Our findings indicate that the entire RTN contains CO_2 -excited neurons and therefore may be involved in the control of breathing, which is consistent with previous work (6,21,23,24,25,31,33,36,37,55,60). Our findings are somewhat at odds with the recent suggestion that there is a specialized region of the caudal RTN that is especially associated with ventilatory control (26,29). We did note that this caudal region appears to be highly vascularized, more so than other areas of the RTN. It may be that some chemosensitive neurons within the RTN are located near blood vessels, as observed in other chemosensitive areas (5), while others are more distant. If this vascular heterogeneity exists, it could contribute to functional differences in sensitivity among neurons that actually share the same intrinsic CO_2 sensitivity. This would make the ventilatory response to CO_2 some weighted average of the PCO_2 in multiple locations in the brain. Therefore, chemoreceptors associated with vessels would respond to rapid changes in CO_2 , and chemoreceptors not associated with vessels would respond to a more stable and slower changing tissue CO_2 level. While this idea is attractive, there appears to be extensive vascularization of the entire RTN with numerous penetrating arteries branching from the basilar artery (40). The relationship between chemosensitive neurons and blood vessels in the RTN warrants further study.

Our results offer insights into the cellular chemosensitive signaling mechanisms as well. It appears that extracellular acidification plays at most a minor role in chemosensitive signaling since RTN neurons were equally excited by hypercapnic acidosis and isohydric hypercapnia. This occurred despite the fact that hypercapnic acidosis induced a larger and more maintained intracellular acidification than isohydric hypercapnia. These findings clearly imply that while intracellular acidification most likely plays a significant role in the chemosensory response, it

is not the sole signal. It is not clear what other intracellular signals are involved in chemosensitive RTN neurons, but the idea that chemosensitivity involves multiple factors has recently been proposed (16,46).

We have made the first simultaneous measurements of V_m and pH_i in astrocytes from chemosensitive brainstem regions. We find no evidence for pH_i recovery in response to hypercapnic acidosis induced acidification. If astrocytes had shown pH_i recovery, and thus caused a larger extracellular acidification, it would have offered a mechanism by which astrocytes could modulate chemosensitivity. However, hypercapnic acidosis may alter astrocyte function in other ways besides intracellular acidification, and this could be the basis for modulation of chemosensitivity by astrocytes. It is also possible that astrocytes are heterogeneous in the RTN and we have studied only one subtype. Finally, we have only studied RTN neurons from neonatal animals. Considerable developmental changes could occur that might result in dramatic changes in chemosensitivity (45). Thus, studies of RTN neurons from adult animals should prove interesting.

Acknowledgements

We thank Phyllis Douglas for technical assistance. This work was supported by National Institutes of Health Grants HL-56683 (RWP) and HL-71001 (JCL and JSE).

References

1. Akilesh MR, Kamper M, Li A, Nattie EE. Effects of unilateral lesions of retrotrapezoid nucleus on breathing in awake rats. *J Appl Physiol* 1997;82:469–479. [PubMed: 9049726]
2. Bayliss DA, Talley EM, Sirois JE, Lei Z. TASK-1 is a highly modulated pH-sensitive “leak” K^+ channel expressed in brain stem respiratory neurons. *Respir Physiol* 2001;129:159–174. [PubMed: 11738652]
3. Belegu RW, Hadjiefendic S, Dreshaj IA, Haxhiu MA, Martin RJ. CO_2 -induced c-fos expression in medullary neurons during early development. *Respir Physiol* 1999;117:13–28. [PubMed: 10505476]
4. Bouyer PG, Bradley SR, Zhao J, Wang W, Richerson GB, Boron WF. Effect of extracellular acid-base disturbances on the intracellular pH of neurones cultured from rat medullary raphé or hippocampus. *J Physiol* 2004;559:85–101. [PubMed: 15194736]
5. Bradley SR, Pieribone VA, Wang W, Severson CA, Jacobs RA, Richerson GB. Chemosensitive serotonergic neurons are closely associated with large medullary arteries. *Nat Neurosci* 2002;5:401–402. [PubMed: 11967547]
6. Coates EL, Li A, Nattie EE. Acetazolamide on the ventral medulla of the cat increases phrenic output and delays the ventilatory response to CO_2 . *J Physiol* 1993;441:433–451. [PubMed: 1816381]
7. Conrad SC, Mulkey DK, Ritucci NA, Dean JB, Putnam RW. Development of chemosensitivity in neurons from the nucleus tractus solitarius (NTS). *FASEB J* 2005;19:A649.
8. Dean JB, Bayliss PA, Erickson JT, Lawing WL, Millhorn DE. Depolarization and stimulation of neurons in nucleus tractus solitarii by carbon dioxide does not require chemical synaptic input. *Neuroscience* 1990;36:207–216. [PubMed: 2120613]
9. Dean JB, Lawing WL, Millhorn DE. CO_2 decreases membrane conductance and depolarizes neurons in the nucleus tractus solitarii. *Exp Brain Res* 1989;76:656–661. [PubMed: 2507342]
10. **Dean JB and Reddy RB** Effects of intracellular dialysis on CO_2/H^+ chemosensitivity in brainstem neurons. In: *Ventral Brainstem Mechanisms and Control of Respiration and Blood Pressure*, edited by Trough CO, Millis RM, Kiwull-Schöne HF, and Schläfke ME. New York: Dekker, 1995, p. 453–461.
11. Deitmer JW, Rose CR. pH regulation and proton signaling by glial cells. *Prog Neurobiol* 1996;48:73–103. [PubMed: 8737439]
12. Duprat F, Lesage F, Fink M, Reyes R, Heurteaux C, Lazdunski M. TASK, a human background K^+ channel to sense external pH variations near physiological pH. *EMBO J* 1997;16:5464–5471. [PubMed: 9312005]

13. Erlichman JS, Cook A, Schwab MC, Thomas WB, Leiter JC. Heterogeneous patterns of pH regulation in glial cells in the dorsal and ventral medulla. *Am J Physiol Regul Integr Comp Physiol* 2003;286:R289–R302. [PubMed: 14525723]
14. Erlichman JS, Li A, Nattie EE. Ventilatory effects of glial dysfunction in a rat brain stem chemoreceptor region. *J Appl Physiol* 1998;85:1599–1604. [PubMed: 9804558]
15. Feldman JL, Mitchell GS, Nattie EE. Breathing: Rhythmicity, plasticity, chemosensitivity. *Annu Rev Neurosci* 2003;26:239–266. [PubMed: 12598679]
16. Filosa JA, Dean JB, Putnam RW. Role of intracellular and extracellular pH in the chemosensitive response of rat locus coeruleus neurons. *J Physiol* 2002;541:493–509. [PubMed: 12042354]
17. Filosa JA, Putnam RW. Multiple targets of chemosensitive signaling in locus coeruleus neurons: role of K^+ and Ca^{2+} channels. *Am J Physiol Cell Physiol* 2002;284:C145–C155. [PubMed: 12388081]
18. Fukuda Y, Honda Y, Schläpke ME, Loeschcke HH. Effect of H^+ on the membrane potential of silent cells in the ventral and dorsal surface layers of the rat medulla in vitro. *Pflügers Arch* 1978;376:229–235.
19. Graß D, Pawlowski PG, Hirrlinger J, Papdopoulos N, Richter DW, Kirchhoff F, Hülsmann S. Diversity of functional astroglial properties in the respiratory network. *J Neurosci* 2004;24:1358–1365. [PubMed: 14960607]
20. Holleran J, Babbie M, Erlichman JS. Ventilatory effects of impaired glial function in a brain stem chemoreceptor region in the conscious rat. *J Appl Physiol* 2001;90:1539–1547. [PubMed: 11247957]
21. Issa FG, Remmers JE. Identification of a subsurface area in the ventral medulla sensitive to local changes in PCO_2 . *J Appl Physiol* 1992;72(2):439–446. [PubMed: 1559917]
22. Largo C, Cuevas P, Somjen GG, Martin del Rio R, Herreras O. The effect of depressing glial function in rat brain in situ on ion homeostasis, synaptic transmission, and neuron survival. *J Neurosci* 1996;16:1219–1229. [PubMed: 8558250]
23. Li A, Nattie EE. Focal central chemoreceptor sensitivity in the RTN studied with a CO_2 diffusion pipette in vivo. *J Appl Physiol* 1997;83(2):420–428. [PubMed: 9262436]
24. Li A, Nattie EE. CO_2 dialysis in one chemoreceptor site, the RTN: stimulus intensity and sensitivity in the awake rat. *Resp Physiol Neurobiol* 2002;133:11–22.
25. Li A, Randall M, Nattie EE. CO_2 microdialysis in the retrotrapezoid nucleus of the rat increases breathing in wakefulness but not in sleep. *J Appl Physiol* 1999;87:910–919. [PubMed: 10484557]
26. Mitchell GS. Back to the future: carbon dioxide chemoreceptors in the mammalian brain. *Nature Neurosci* 2004;7(12):1288–1290. [PubMed: 15643436]
27. Mitchell RA, Loeschcke HH, Massion WH, Severinghaus JW. Respiratory responses mediated through superficial chemosensitive areas on the medulla. *J Appl Physiol* 1963;18:523–533.
28. Mulkey DK, Henderson RA, Ritucci NA, Putnam RW, Dean JB. Oxidative stress decreases pH_i and Na^+/H^+ exchange and increases excitability of solitary complex neurons from rat brain slices. *Am J Physiol Cell Physiol* 2004;286:C940–C951. [PubMed: 14668260]
29. Mulkey DK, Stornetta RL, Weston MC, Simmons JR, Parker A, Bayliss DA, Guyenet PG. Respiratory control by ventral surface chemoreceptor neurons in rats. *Nature Neurosci* 2004;7(12):1360–1369. [PubMed: 15558061]
30. Nattie EE. CO_2 , brainstem chemoreceptors and breathing. *Prog Neurobiol* 1999;59:299–331. [PubMed: 10501632]
31. Nattie EE, Fung M-L, Li A, St. John WM. Responses of respiratory modulated and tonic units in the retrotrapezoid nucleus to CO_2 . *Resp Physiol* 1993;94:35–50.
32. Nattie EE, Li A. Fluorescent location of RVLN kainate microinjections that alter the control of breathing. *J Appl Physiol* 1990;68:1157–1166.
33. Nattie EE, Li A. Retrotrapezoid nucleus lesions decrease phrenic activity and CO_2 sensitivity in rats. *Resp Physiol* 1994;97:63–77.
34. Nattie EE, Li A, St. John WM. Lesions in retrotrapezoid nucleus decrease ventilatory output in anesthetized or decerebrated cats. *J Appl Physiol* 1991;71:1364–1375. [PubMed: 1757359]
35. Nottingham S, Leiter JC, Wages P, Buhay S, Erlichman JS. Developmental changes in intracellular pH regulation in medullary neurons of the rat. *Am J Physiol Regul Integr Comp Physiol* 2001;281:R1940–R1951. [PubMed: 11705781]

36. Okada Y, Chen Z, Jiang W, Kuwana SI, Eldridge FL. Anatomical arrangement of hypercapnia-activated cells in the superficial ventral medulla of rats. *J Appl Physiol* 2002;93:427–439. [PubMed: 12133847]
37. Onimaru H, Arata A, Homma I. Firing properties of respiratory rhythm generating neurons in the absence of synaptic transmission in rat medulla in vitro. *Exp Brain Res* 1989;76:530–536. [PubMed: 2551710]
38. Oyamada Y, Ballantyne D, Mückenhoff K, Scheid P. Respiration-modulated membrane potential and chemosensitivity of locus coeruleus neurones in the in vitro brainstem-spinal cord of the neonatal rat. *J Physiol* 1998;513:381–398. [PubMed: 9806990]
39. Pappas CA, Ransom BR. Depolarization-induced alkalization (DIA) in rat hippocampal astrocytes. *J Neurophysiol* 1994;72:2816–2826. [PubMed: 7897491]
40. **Paxinos G.** *The Rat Nervous System*, 2nd Edition. New York: Academic Press, pp. 8–10, 1995.
41. **Paxinos G and Watson C** The rat brain in stereotaxic coordinates. Third edition. San Diego: Academic Press, 1997.
42. Pearce RA, Stornetta RL, Guyenet PG. Retrotrapezoid nucleus in the rat. *Neurosci Lett* 1989;101:138–142. [PubMed: 2771161]
43. Peters O, Schipke CG, Hashimoto Y, Kettenmann H. Different mechanisms promote astrocyte Ca^{2+} waves and spreading depression in the mouse neocortex. *J Neurosci* 2003;23(30):9888–9896. [PubMed: 14586018]
44. Pineda J, Aghajanian GK. Carbon dioxide regulates the tonic activity of locus coeruleus neurons by modulating a proton- and polyamine-sensitive inward rectifier potassium current. *Neuroscience* 1997;77:723–743.
45. **Putnam RW, Conrad SC, Gdovin MJ, Erlichman JS,** and Leiter JC. Neonatal maturation of the hypercapnic ventilatory response and central neural CO_2 chemosensitivity. *Respir Physiol Neurobio* IN PRESS, 2005.
46. Putnam RW, Filosa JA, Ritucci NA. Cellular mechanisms involved in CO_2 and acid signaling in chemosensitive neurons. *Am J Physiol Cell Physiol* 2004;287:C1493–1526. [PubMed: 15525685]
47. Putnam RW, Ritucci NA, Erlichman JS, Leiter JC. The effects of hypercapnia on membrane potential (V_m) and intracellular pH (pH_i) in neurons and astrocytes from the retrotrapezoid nucleus (RTN). *FASEB J* 2005;19:A647.
48. Ransom BR. Glial modulation of neural excitability mediated by extracellular pH: a hypothesis. *Prog Brain Res* 1992;94:37–46. [PubMed: 1287724]
49. Richerson GB. Response to CO_2 of neurons in the rostral ventral medulla in vitro. *J Neurophysiol* 1995;73:933–944. [PubMed: 7608778]
50. **Richerson GB** Cellular mechanisms of sensitivity to pH in the mammalian respiratory system. In: *pH and Brain Function*, edited by Kaila K and Ransom BR. New York: Wiley-Liss, 1998, p. 509–533.
51. Ritucci NA, Dean JB, Putnam RW. Intracellular pH response to hypercapnia in neurons from chemosensitive areas of the medulla. *Am J Physiol Regul Integr Comp Physiol* 1997;273:R433–R441.
52. Ritucci NA, Erlichman JS, Temkin M, Leiter JC, Putnam RW. Effects of hypercapnia on membrane potential (V_m) and intracellular pH (pH_i) in neurons and glia from the retrotrapezoid nucleus (RTN). *FASEB J* 2004;18(5):A1062.
53. Ritucci NA, Putnam RW, Dean JB. Simultaneous measurement of intracellular pH and membrane potential in locus coeruleus neurons during hypercapnia. *FASEB J* 1999;13:A163.
54. **Rose CR and Ransom BR.** pH regulation in mammalian glia. In: *pH and Brain Function*, edited by Kaila K and Ransom BR. New York: Wiley-Liss, 1998, pp. 253–275.
55. Sato M, Severinghaus JW, Basbaum AI. Medullary CO_2 chemoreceptor neuron identification by c-fos immunocytochemistry. *J Appl Physiol* 1992;73:96–100. [PubMed: 1506406]
56. Shrode LD, Putnam RW. Intracellular pH regulation in primary rat astrocytes and C6 glioma cells. *Glia* 1994;12:196–210. [PubMed: 7851988]
57. Smith JC, Morrison DE, Ellenberger HH, Otto MR, Feldman JL. Brainstem projections to the major respiratory neuron populations in the medulla of the cat. *J Comp Neurol* 1989;281:69–96. [PubMed: 2466879]

58. Stunden CE, Filosa JA, Garcia AJ, Dean JB, Putnam RW. Development of in vivo ventilatory and single chemosensitive neuron responses to hypercapnia in rats. *Resp Physiol* 2001;127:135–155.
59. Summers BA, Overholt JL, Prabhakar N. CO₂ and pH independently modulate L-type Ca²⁺ current in rabbit carotid body glomus cells. *J Neurophysiol* 2002;88:604612.
60. Teppema LJ, Veening JG, Kranenburg A, Dahan A, Berkenbosch A, Olievier C. Expression of c-fos in the rat brainstem after exposure to hypoxia and to normoxic and hyperoxic hypercapnia. *J Comp Neurol* 1997;388:169–190. [PubMed: 9368836]
61. Trapp S, Lückermann M, Brooks PA, Ballanyi K. Acidosis of rat dorsal vagal neurons in situ during spontaneous and evoked activity. *J Physiol* 1996;496:695–710. [PubMed: 8930837]
62. Wallraff A, Odermatt B, Willecke K, Steinhäuser C. Distinct types of astroglial cells in the hippocampus differ in gap junction coupling. *Glia* 2004;48:36–43. [PubMed: 15326613]
63. Wang W, Bradley SR, Richerson GB. Quantification of the response of rat medullary raphé neurons to independent changes in pH_o and P_{CO2}. *J Physiol* 2002;540:951–970. [PubMed: 11986382]
64. Wang W, Pizzonia JJ, Richerson GB. Chemosensitivity of rat medullary raphe neurons in primary tissue culture. *J Physiol* 1998;511:433–450. [PubMed: 9706021]
65. Washburn CP, Sirois JE, Talley EM, Guyenet P, Bayliss DA. Serotonergic raphe neurons express TASK channel transcripts and a TASK-like pH- and halothane-sensitive K⁺ conductance. *J Neurosci* 2002;22:1256–1265. [PubMed: 11850453]
66. Wellner-Kienitz MC, Shams H, Scheid P. Contribution of Ca²⁺- activated K⁺ channels to Central chemosensitivity in cultivated neurons of fetal rat medulla. *J Neurophysiol* 1998;79:2885–2894. [PubMed: 9636094]
67. Wickström R, Höckfelt T, Lagercrantz H. Development of CO₂-response in the early newborn period in rat. *Resp Physiol Neurobiol* 2002;132:145–158.
68. Wu J, Shen W, Jiang C. Expression and coexpression of CO₂-sensitive Kir channels in brainstem neurons of rats. *J Memb Biol* 2004;197:179–191.

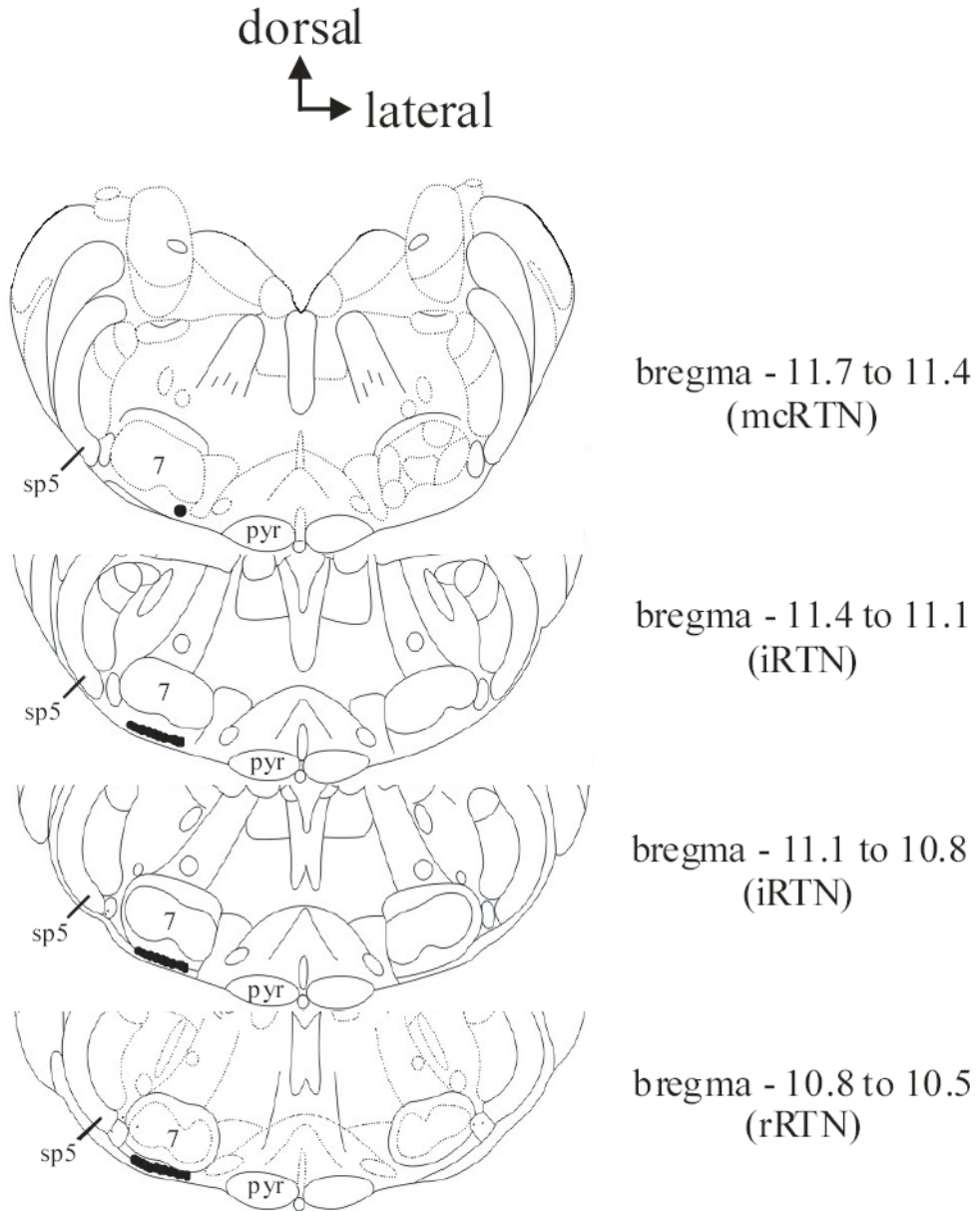


Figure 1. Medullary slices indicating mcRTN and irRTN areas.

The level in relation to bregma is indicated to the right of each medullary slice. The top, most caudal slice contains the mcRTN and the bottom three intermediate (iRTN) and rostral (rRTN) slices contain the irRTN. Dark circle ventral and at the medial aspect of the facial nucleus in the top most caudal slice indicates the area of the mcRTN where recordings were performed. Dark shaded areas ventral to the facial nucleus in the bottom three slices indicates the areas of the irRTN where recordings were performed. Pyr = pyramids; 7 = facial nucleus; sp5 = spinal trigeminal tract. Figures modified from Paxinos and Watson (41).

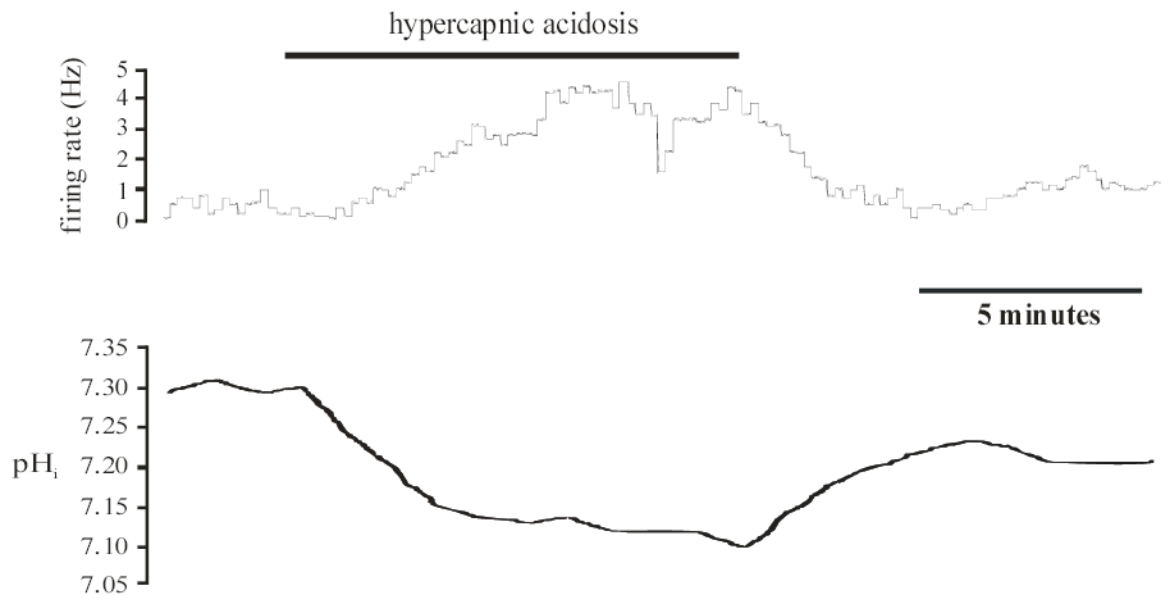


Figure 2. Hypercapnic acidosis-excited mcRTN neuron

Top panel: Integrated firing rate trace of an individual mcRTN neuron. Hypercapnic acidosis (10% CO₂, pH_o 7.15) resulted in an increase in firing rate that returned towards its initial value upon return to control solution (5% CO₂, pH_o 7.45). Bottom panel: pH_i trace of the same neuron in the top panel. Hypercapnic acidosis resulted in a maintained, intracellular acidification that returned towards its initial value under control conditions.

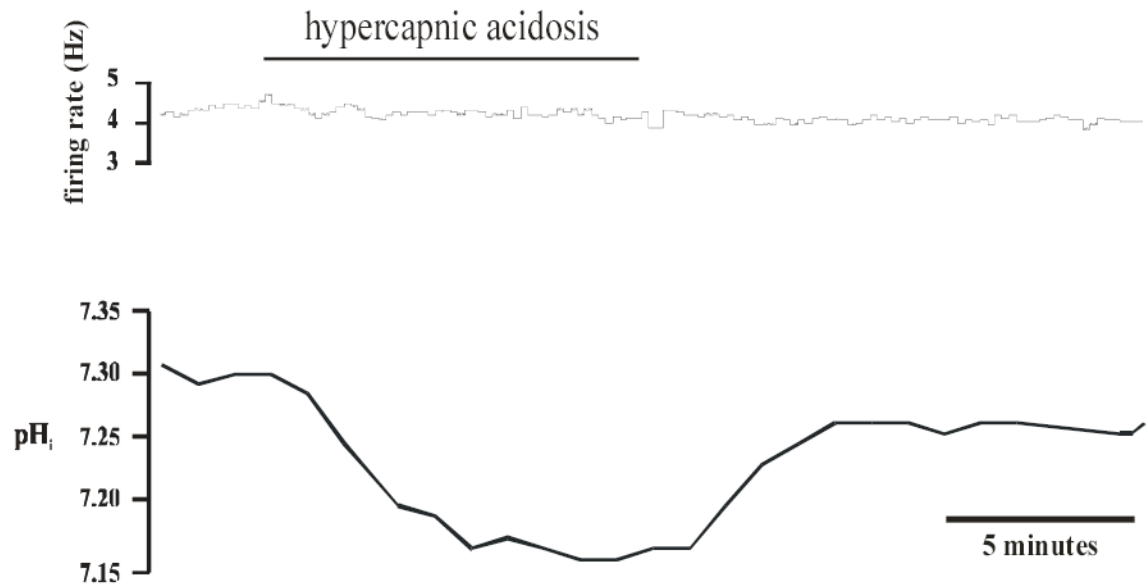


Figure 3. Hypercapnic acidosis-insensitive mcRTN neuron

Top panel: Integrated firing rate trace of an individual mcRTN neuron. Firing rate did not change before, during or after hypercapnic acidosis exposure. Bottom panel: pH_i trace of the same neuron in the top panel. Hypercapnic acidosis (10% CO₂, pH_o 7.15) resulted in a maintained, intracellular acidification that returned towards its initial value under control conditions (5% CO₂, pH_o 7.45).

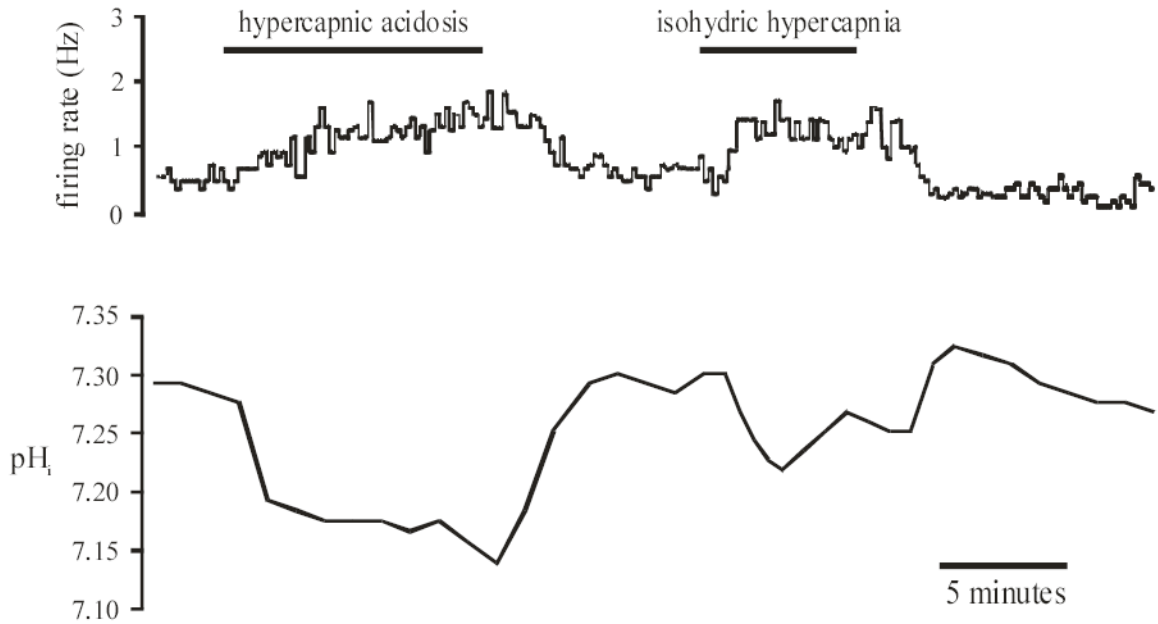


Figure 4. mcRTN neuron excited by both hypercapnic acidosis and isohydric hypercapnia

Top panel: Integrated firing rate trace of an individual mcRTN neuron. Hypercapnic acidosis (10% CO₂, pH_o 7.15) resulted in an increase in firing rate that returned towards its initial value upon return to control solution (5% CO₂, pH_o 7.45). Isohydric hypercapnia (in the same neuron) again resulted in a maintained increase in firing rate that returned towards its initial value upon return to control solution. Bottom panel: pH_i trace of the same neuron in the top panel. Hypercapnic acidosis resulted in a maintained, intracellular acidification that returned towards its initial value upon return to control solution (5% CO₂, pH_o 7.45). Isohydric hypercapnia resulted in an initial, intracellular acidification followed by pH_i recovery. Upon return to control solution, pH_i overshoot its initial value, further indicating pH_i recovery during isohydric hypercapnia. pH_i then returned towards its initial value.

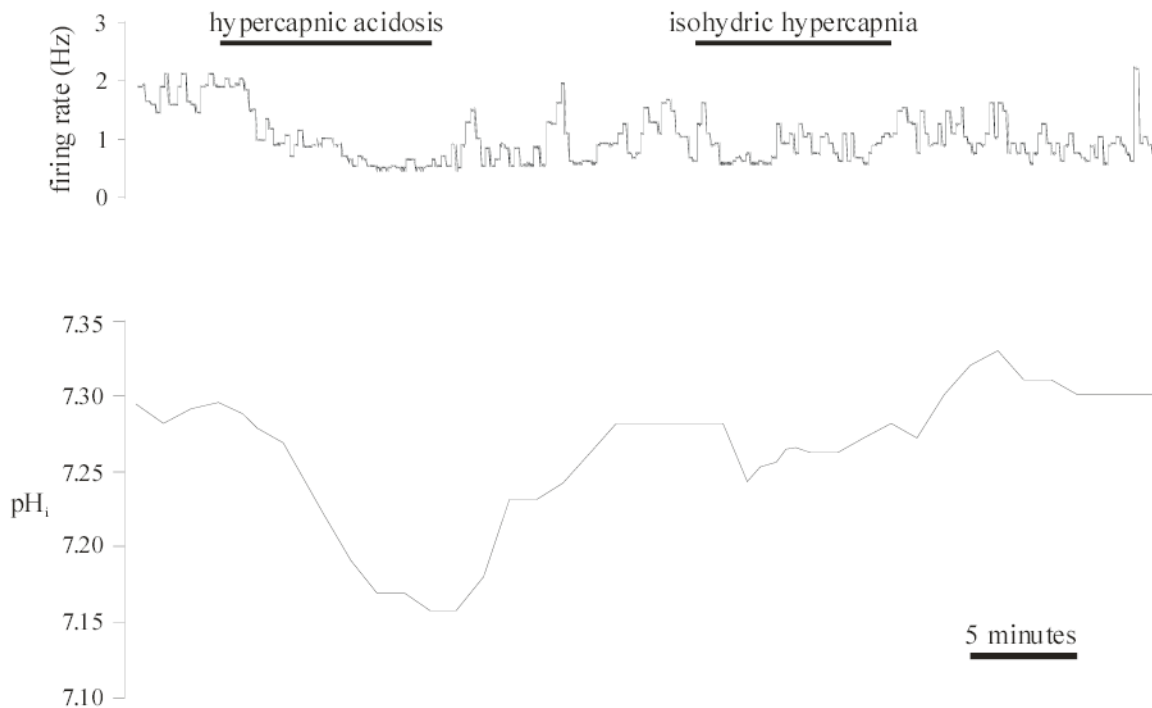


Figure 5. mcRTN neurons insensitive to both hypercapnic acidosis and isohydric hypercapnia

Top panel: Integrated firing rate trace of an individual mcRTN neuron. Average integrated firing rate was 1.8 Hz before exposure to and decreased (0.5 Hz) upon exposure to hypercapnic acidosis (10% CO₂, 26 mM HCO₃⁻, pH_o 7.15). However, this effect was not reversible, firing rate remaining at 0.6 Hz upon return to control (5% CO₂, pH_o 7.45) solution. Exposure to isohydric hypercapnia (10% CO₂, 52 mM HCO₃⁻, pH_o 7.45) did not change firing rate (0.8 Hz) nor did return to control solution (0.9 Hz). Bottom panel: pH_i trace of the same neuron in the top panel. Hypercapnic acidosis resulted in a maintained, intracellular acidification that returned towards its initial value upon return to control solution (5% CO₂, 26 mM HCO₃⁻, pH_o 7.45). Isohydric hypercapnia resulted in an initial, intracellular acidification followed by pH_i recovery. Upon return to control solution, pH_i overshoot its initial value, further indicating pH_i recovery during isohydric hypercapnia. pH_i then returned towards its initial value.

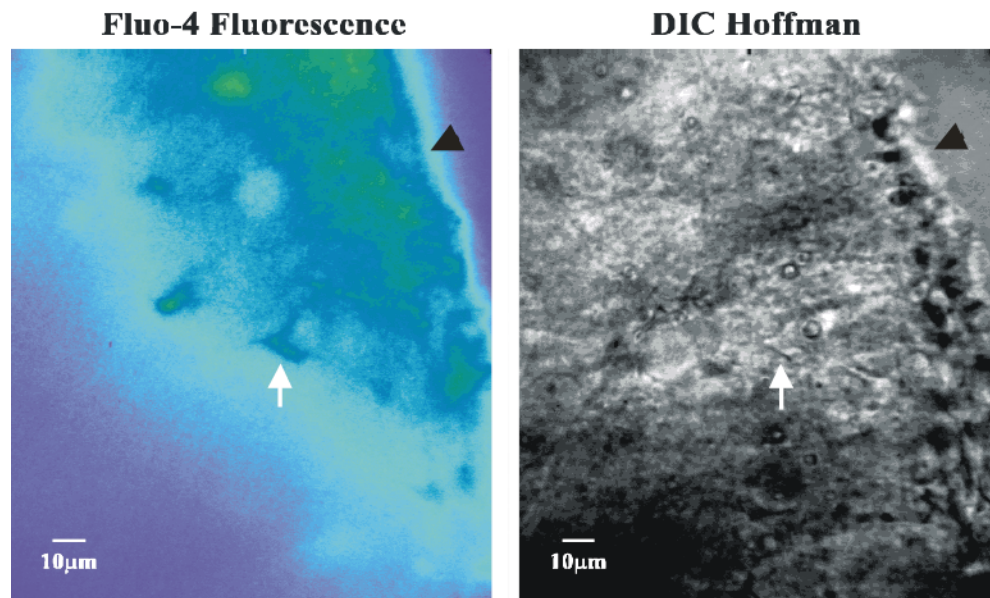


Figure 6. Fluo-4 fluorescence and Hoffman contrast images of the irRTN

Left panel: Fluo-4 fluorescence image of the irRTN. Fluorescence image of a slice loaded with the fluorescent dye, fluo-4, which preferentially loads glia. White arrow points at a fluo-4 loaded cell. Black arrow head points to the ventrolateral surface. Right panel: Hoffman contrast image of the same area shown in the left panel. White arrow points at the same cell as in the left panel. This cell was patched and the V_m and pH_i traces shown in Figure 7. Black arrow head points to the ventrolateral surface. Note how close to the ventral surface the cells of the RTN are located.

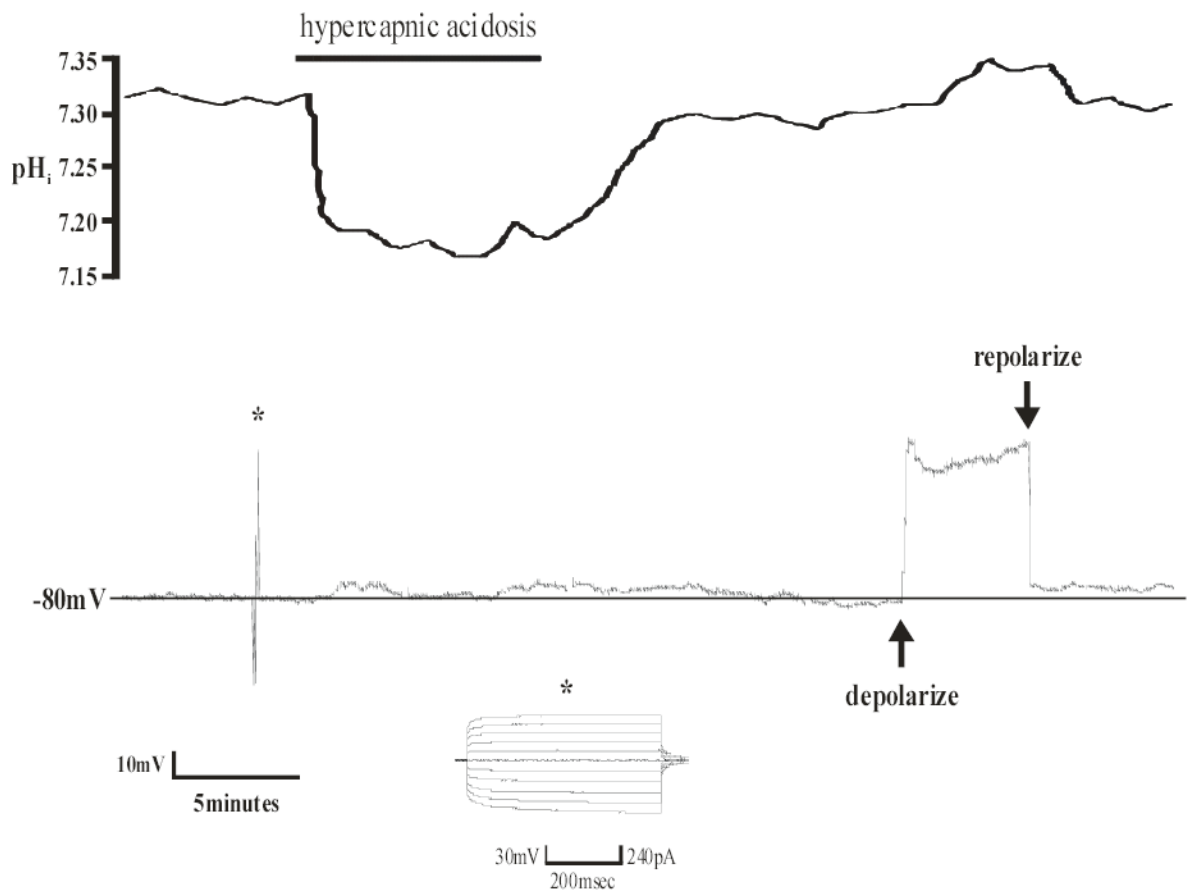


Figure 7. Response to hypercapnic acidosis of an astrocyte from the irRTN

Top panel: pH_i trace of an individual astrocyte from the irRTN. Hypercapnic acidosis resulted in a maintained, intracellular acidification that returned towards its initial value upon return to control solution. Bottom panel: V_m trace of the same astrocyte in the top panel. Hypercapnic acidosis (10% CO₂, pH_o 7.15) caused a depolarization of approximately 5mV, which returned towards normal under control conditions (5% CO₂, pH_o 7.45). Note that the changes in V_m follow the changes in pH_i. Also note the hyperpolarized V_m (-80mV) and the lack of action potentials, both of which indicate this is an astrocyte. Asterisk indicates a pulse protocol (generated by p-Clamp software) showing that positive current is unable to elicit action potentials, which is further proof that this cell is an astrocyte. At the end of each of these experiments, depolarizing DC current (~ +40mV) was continuously injected via the Dagan amplifier resulting in an intracellular alkalinization (see top panel), which is known as depolarization-induced alkalinization (39). This is additional evidence that this cell is an astrocyte.